SEMARAK ILMU PUBLISHING

Journal of Advanced Research in Applied Mechanics

Journal homepage:
https://semarakilmu.com.my/journals/index.php/appl_mech/index
ISSN: 2289-7895

Effect of Material Properties on the Behaviour of Cross-Ply Laminated Cylindrical Shells under Thermo-Mechanical Load

Nur Amalina Pakry[1], Mohamed Ali Jaffar Syed[1,*], M.S.I. Shaik Dawood[1], Hanan Mokhtar[1]

[1] Department of Mechanical and Aerospace Engineering, Kulliyyah of Engineering, International Islamic University Malaysia, Gombak, 53100 Kuala Lumpur, Malaysia

ARTICLE INFO

Article history:
Received 17 October 2023
Received in revised form 19 December 2023
Accepted 6 January 2024
Available online 23 February 2024

Keywords:
Thermo-mechanical; composite laminates; cylindrical shells; elasticity solution; material properties

ABSTRACT

Aerodynamic heating is a concern for aerospace structures such as composite laminated shells. A structure which is under axial and bending stress due to mechanical loading might fail if the design process does not consider the possibility of additional stress due to thermal load. This work aims to develop 3D elasticity solution for composite laminated shell under thermo-mechanical loading and analyse the effect of material properties. In this work, 3D linear uncoupled thermo-elasticity solution was developed for thermal bending of simply supported laminated composite cylindrical shell under cylindrical bending. The results from the analysis were validated against the existing benchmark solution for both mechanical loading and thermal loading. Useful results for cylindrical shells under thermal loading were presented for three different composite laminate materials at different thicknesses in tabular and graphical form. It is expected that the benchmark results presented herein will serve as reference to select an accurate higher order model for stress analysis of composite laminates under thermo-mechanical loading.

1. Introduction

Structures of aerospace vehicles experience thermal load in addition to mechanical load due to aerodynamic heating. These structures are mostly assembled from composite laminates due to their high specific modulus and strength with low thermal expansion coefficient properties. Thus, the analysis of composite shell structure under thermo-mechanical loading has been an area of interest for researchers. Among the theories used for analysis, elasticity solution is the most valuable as it represents a realistic and closer approximation to the actual behavior of the structures. Hence, it serves as a benchmark in order to determine the range of applicability of classical and refined engineering theories.

Previously Ren [1] had developed the elasticity solution for cylindrical bending of laminate cylindrical shell under mechanical load. Huang and Tauchert [2,3] further developed an elasticity solution for simply supported cylindrical cross-ply panels and doubly curved cross-ply laminate under

* *Corresponding author.*
Email address: jaffar@iium.edu.my

https://doi.org/10.37934/aram.114.1.5165

thermo-mechanical loading. Khdeir *et al.,* [4] conducted a thermoelastic analysis of laminate shell using higher shear deformation theory and compared the result with first deformation theory and classical theory. Bhaskar *et al.,* [5] presented elasticity solution for plates under thermal loading. Khare *et al.,* [6] provided thermo-mechanical analysis of laminate shell by using 2D higher order theory. Qian *et al.,* [7] developed elasticity solution for laminated arch and Ali *et al.,* [8] studied the effect of hygrothermal load on cylindrical shell and developed new higher order theory for the analysis. Liu *et al.,* [9] used finite element method to do a 3D thermoelastic analysis of laminated plates and shells. Kumari and Kar [10,11] presented a 3D solution for both cross-ply and angle-ply cylindrical shell for arbitrary boundary condition using Kantorovich method. Yang *et al.,* [12] analyzed curved laminate composite shell using finite element method based on layer-wise theory with linear expansion. Soumen *et al.,* [13] used finite element method to analyze laminate composite shell based on higher order zigzag theory. Sandipan and Chaitali [14] made a static analysis using finite element for moderately thick hyperbolic paraboidal laminated shell. Andreas and Christian [15] applied closed form solution, layer-wise theory, and a semi-analytical approach to analyze cylindrically curved cross-ply laminated shell under transverse loading.

Research was also done to study the behavior of composite laminate under various boundary conditions. Chandrashekhara and Bhimaraddi [16] covered the deflection of laminate panels for different layups and boundary conditions under thermal loading using finite element model. Sharvari *et al.,* [17] studied normalized stresses and displacements of unidirectional, bidirectional and symmetrical composite laminate shells under different mechanical loadings by using elasticity solution. Alibeigloo and Shakeri [18] investigated behavior of cross-ply laminate cylindrical panel with various edge conditions subjected to static radial load by using differential quadrature method. Biswal *et al.,* [19] produced experimental numerical results on change in elasticity modulus of composite laminate with increasing temperature. Amoushahi and Goodarzi [20] discovered the effect of changing material properties of laminate plates due to various temperature on natural frequency and buckling factor by using finite strip formulations. From the literature, it can be found that study on composite laminates under thermo-mechanical loading is still an active area of research and many new higher order model are being proposed for analysis. In this work, elasticity solution for simply supported cylindrical shells under thermo-mechanical loading was developed and the effect of material properties on the behavior of cylindrical shells is studied which will serve as a benchmark to develop new higher order model.

2. Methodology

An orthotropic N-layer cylindrical shell that was infinitely long in the z direction as shown in Figure 1 was considered. The analysis was simplified to be a cylindrical bending problem hence $\varepsilon_z = 0$. Transverse mechanical load q that has a sinusoidal distribution along θ is applied on the top surface. Similarly thermal load $T(r, \theta)$ considered, has a sinusoidal distribution along θ and linearly varying across the thickness. Mean radius of the shell is R, while total thickness of shell was assumed to be h and angle θ ranged from 0 to φ.

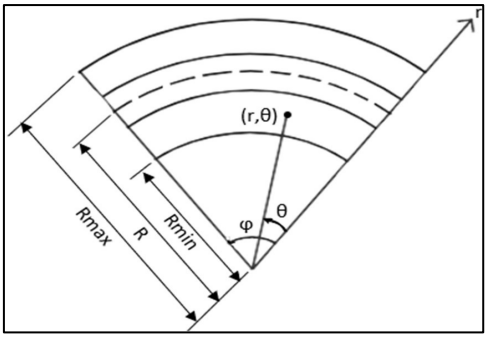

Fig. 1. Geometry and coordination of laminated cylindrical shells

2.1 Formulation

To evaluate the displacement and stresses of a orthotropic N-layer cylindrical shell under thermo-mechanical loading, the procedure demonstrated by Ren [1] and Ali *et al.,* [8] was adopted. Equilibrium equation Eq. (1), thermoelastic stress-strain law Eq. (2) and strain-displacement relation Eq. (3) formed the governing equations for the elasticity solution. C_{ij} represented the stiffness coefficients with respect to stress-free state (i,j = 1 ~ 6). For cross-ply shells, $C_{14} = C_{24} = C_{34} = C_{56} = 0$. α_i and T represented thermal expansion coefficient and temperature difference respectively.

$$\frac{d\sigma_r}{dr} + \frac{1}{r}\frac{d\tau_{r\theta}}{d\theta} + \frac{\sigma_r - \sigma_\theta}{r} = 0$$
$$\frac{d\tau_{r\theta}}{dr} + \frac{1}{r}\frac{d\sigma_\theta}{d\theta} + \frac{2\tau_{r\theta}}{r} = 0 \quad (1)$$

$$\begin{Bmatrix}\sigma_r\\ \sigma_\theta\\ \sigma_z\end{Bmatrix} = \begin{bmatrix}C_{rr} & C_{r\theta} & C_{rz}\\ C_{r\theta} & C_{\theta\theta} & C_{\theta z}\\ C_{rz} & C_{\theta z} & C_{zz}\end{bmatrix}\begin{Bmatrix}\varepsilon_r - \alpha_r T\\ \varepsilon_\theta - \alpha_\theta T\\ -\alpha_z T\end{Bmatrix} \quad (2)$$

$$\tau_{r\theta} = C_{r\theta}\gamma_{r\theta}$$
$$\varepsilon_r = \frac{u_r}{r}$$
$$\varepsilon_\theta = \frac{u_r}{r} + \frac{1}{r}\frac{u_\theta}{\theta} \quad (3)$$
$$\gamma_{r\theta} = \frac{1}{r}\frac{u_r}{\theta} - \frac{u_\theta}{r}$$

By substituting Eq. (2) and Eq. (3) into Eq. (1), characteristic equation Eq. (4) was obtained. u_r and u_θ were displacements in the *r* and θ direction respectively.

$$C_{11}\frac{d^2u_r}{dr^2} + \frac{C_{55}}{r^2}\frac{d^2u_r}{d\theta^2} + \frac{C_{12}+C_{55}}{r}\frac{d^2u_\theta}{drd\theta} + \frac{C_{11}}{r}\frac{du_r}{dr} - \left(\frac{C_{22}+C_{15}}{r^2}\frac{du_\theta}{d\theta}\right) - \frac{C_{22}}{r^2}u_r \quad (4)$$
$$= (C_{11}\alpha_r + C_{12}\alpha_\theta + C_{13}\alpha_z)\frac{dT}{dr} + (C_{11}\alpha_r + C_{12}\alpha_\theta + C_{13}\alpha_z)\frac{1}{r} - (C_{12}\alpha_r + C_{22}\alpha_\theta + C_{23}\alpha_z)\frac{1}{r}$$

$$C_{55}\frac{d^2u_\theta}{dr^2}+\frac{C_{22}}{r^2}\frac{d^2u_\theta}{d\theta^2}+\frac{C_{12}+C_{55}}{r}\frac{d^2u_r}{drd\theta}+\frac{C_{55}}{r}\frac{du_\theta}{dr}+\frac{C_{22}+C_{55}}{r^2}\frac{du_r}{d\theta}-\frac{C_{55}}{r^2}u_\theta$$
$$=(C_{12}\alpha_r+C_{22}\alpha_\theta+C_{23}\alpha_z)\frac{dT}{d\theta}$$

The laminate shell was assumed to be simply supported along the longitudinal edges.

$$\text{At } \theta=0,\varphi \qquad u_r=\sigma_\theta=0 \tag{5}$$

The following solutions where Ψ_r and Ψ_θ as functions of *r* were assumed to satisfy the condition in Eq. (5).

$$u_r=\psi_r\sin\frac{m\pi\theta}{\varphi}$$
$$u_\theta=\psi_\theta\cos\frac{m\pi\theta}{\varphi} \tag{6}$$

As the cylindrical shell was under thermo-mechanical loading, temperature loading and mechanical loading were expressed as:

$$T=T(r)\sin s\theta \tag{7}$$

$$\text{At } r=R_{max} \qquad \sigma_r=q\sin s\theta \tag{8}$$

where $s=\frac{m\pi\theta}{\varphi}$ and $m=1$.

2.2 Solution

When Eq. (6) was substituted into Eq. (4), a set of second order system of ordinary differential equations was formed.

$$\left[C_{11}\left(\frac{d}{dr}\right)^2+\frac{C_{55}}{r}s^2+\frac{C_{11}}{r}\left(\frac{d}{dr}\right)-\frac{C_{22}}{r^2}\right]\Psi_r+\left[\left(\frac{C_{22}+C_{55}}{r^2}\right)s-\left(\frac{C_{12}+C_{55}}{r}\right)s\left(\frac{d}{dr}\right)\right]\Psi_\theta$$
$$=(C_{11}\alpha_r+C_{12}\alpha_\theta+C_{13}\alpha_z)\alpha_L\frac{dT}{dr}+(C_{11}\alpha_r+C_{12}\alpha_\theta+C_{13}\alpha_z)\alpha_L\frac{T}{r}-(C_{12}\alpha_r+C_{22}\alpha_\theta+C_{23}\alpha_z)\alpha_L\frac{T}{r}$$
$$\left[\left(\frac{C_{12}+C_{55}}{r}\right)s\left(\frac{d}{dr}\right)+\left(\frac{C_{22}+C_{55}}{r^2}\right)s\right]\Psi_r+\left[C_{55}\left(\frac{d}{dr}\right)^2-\frac{C_{22}}{r^2}s^2+\frac{C_{55}}{r}\left(\frac{d}{dr}\right)-\frac{C_{55}}{r^2}\right]\Psi_\theta$$
$$=(C_{12}\alpha_r+C_{22}\alpha_\theta+C_{23}\alpha_z)\frac{\alpha_L}{r}sT \tag{9}$$

The equations were further simplified into matrix form as shown in Eq. (11) by using Eq. (10).

$$r=e^{\ln r} \qquad \ln r=t \qquad D=\frac{d}{dt} \tag{10}$$

$$[P]\begin{Bmatrix}\Psi_r\\ \Psi_\theta\end{Bmatrix}=\{Q\} \tag{11}$$

where $[P] = \begin{bmatrix} A_1D^2 - A_2 & A_3 - A_4D \\ A_4D + A_3 & A_5D^2 - A_6 \end{bmatrix}$

$A_1 = C_{11},\ A_2 = C_{55}s^2 + C_{22},\ A_3 = (C_{22} + C_{55})s,\ A_4 = (C_{12} + C_{55})s,\ A_5 = C_{55},$

$A_6 = C_{22}s^2 + C_{55}$

$$\{Q\} = \begin{Bmatrix} (C_{11}\alpha_r + C_{12}\alpha_\theta + C_{13}\alpha_z)D + \left(C_{11} - C_{12})\alpha_r + (C_{12} - C_{22})\alpha_\theta + (C_{13 - C_{23}})\alpha_z\right) \\ (C_{12}\alpha_r + C_{22}\alpha_\theta + C_{23}\alpha_z)s \end{Bmatrix} \alpha_L e^t T$$

Since the equations were nonhomogeneous, the solutions were written in terms of complementary and particular solutions.

$$\Psi_r = \Psi_{rc} + \Psi_{rp}$$
$$\Psi_\theta = \Psi_{\theta c} + \Psi_{\theta p} \quad (12)$$

The subscript *c* and *p* represented complementary solution and particular solution respectively.

2.2.1 Complementary solution

The solution of Eq. (11) was taken to be:

$$\begin{Bmatrix} \Psi_{rc} \\ \Psi_{\theta c} \end{Bmatrix} = \begin{Bmatrix} k_1 \\ k_2 \end{Bmatrix} e^{\lambda t} \quad (13)$$

For complementary solution, Eq. (13) was substituted into Eq. (11) and $\{Q\} = 0$. By solving the quadratic equation of $A\lambda^2 + B\lambda + C = 0$, values of λ_j were obtained. Hence Ψ_{rc} and $\Psi_{\theta c}$ were written as in Eq. (14) where G_j and H_j were undetermined constants and F_{ij} and S_{ij} were functions of r.

$$\Psi_{rc} = \sum_{j=1}^{2N}\left[F_{rj}G_j + S_{rj}H_j\right]$$
$$\Psi_{\theta c} = \sum_{j=1}^{2N}\left[F_{\theta j}G_j + S_{\theta j}H_j\right] \quad (14)$$

For an *N*-layer shell, there were *4N* constants. The values of the constants were found by using the conditions in Eq. (5) and Eq. (8) as well as the interface continuity condition.

2.2.2 Particular solution

For mechanical loading, the right hand side of characteristic equation Eq. (4) would be zero. Hence, elasticity solution for laminate shell under mechanical loading would be obtained at the end of section 2.2.1. However, for thermal loading the right hand side of Eq. (4) contained a value thus particular solution had to be calculated. The temperature distribution was assumed to be linear across the thickness from T_0 at $r = R_{max}$ to $-T_0$ at $r = R_{min}$.

The linear temperature distribution was introduced to Eq. (11). Two sets of solutions were assumed.

$$v_1 = \begin{Bmatrix} a_1 \\ a_2 \end{Bmatrix} e^t, m \neq 1$$
$$v_2 = \begin{Bmatrix} b_1 \\ b_2 \end{Bmatrix} e^{2t}, m \neq 2 \quad (15)$$

Substituting Eq. (15) into Eq. (11) where $\lambda = [1 \quad 2]$ and $\Psi = [v_1 \quad v_2]$ respectively gave Eq. (16).

$$[P(\lambda)] \begin{Bmatrix} v_1 \\ v_2 \end{Bmatrix} = \begin{Bmatrix} f_1 e^t \\ f_2 e^{2t} \end{Bmatrix} \quad (16)$$

where f_1 and f_2 were functions of α_L and T. Thus, the particular solution can be written as:

$$\Psi_{rp} = a_1 e^t + b_1 e^{2t}$$
$$\Psi_{\theta p} = a_2 e^t + b_2 e^{2t} \quad (17)$$

Elasticity solution for laminated shell under thermo-mechanical loading could be obtained by substituting Eq. (12) into Eq. (6) to get displacements. MATLAB code was developed based on the elasticity solution and used to generate the results in Section 3.

3. Results and Discussion

3.1 Validation of Elasticity Solution

The laminates were assumed to have the same thickness and were of the same orthotropic material, Graphite/Epoxy. The material properties were recorded in Table 1. *T* and *L* referred to the properties perpendicular and parallel to the fiber orientation respectively. The laminates were taken to be simply supported. Results are regenerated based on the developed elasticity solution for cylindrical shell strips under mechanical and thermal loading. The results were validated against benchmark results from Ren [1] as shown in Table 2 for mechanical loading and validated against Ali *et. al.*[8] for thermal loading as shown in Table 3. The results were normalized by using the following dimensionless expressions:

Mechanical [1]:

$$\overline{u_r} = \frac{10E_T u_r}{qhS^4} \qquad \overline{u_\theta} = \frac{10E_T u_\theta}{qhS^4} \qquad \overline{\tau_{r\theta}} = \frac{\tau_{r\theta}}{qS}$$

$$\overline{\sigma_\theta} = \frac{\sigma_\theta}{qS} \qquad \overline{\sigma_x} = \frac{\sigma_x}{qS} \qquad \overline{\sigma_z} = \frac{\sigma_z}{\sigma_x(R_{max}\frac{\varphi}{2})}$$

$$S = \frac{R}{h} \qquad \bar{z} = \frac{z}{h}$$

Thermal [8]:

$$\overline{u_r} = \frac{u_r}{h\alpha_L T_0 S^2} \qquad \overline{u_\theta} = \frac{u_\theta}{h\alpha_L T_0 S}$$

$$\overline{\tau_{r\theta}} = \frac{\tau_{r\theta}}{E_T \alpha_L T_0} \qquad \overline{\sigma_\theta} = \frac{\sigma_\theta}{E_T \alpha_L T_0} \qquad S = \frac{R}{h}$$

Table 1
Material Properties of Graphite/Epoxy Laminate

$E_L(psi)$	$E_T(psi)$	$G_{LT}(psi)$	$G_{TT},(psi)$	$\nu_{LT} = \nu_{TT}$	$\frac{\alpha_T}{\alpha_L}$
25 x 10^6	1 x 10^6	0.5 x 10^6	0.2 x 10^6	0.25	1125

Table 2
Dimensionless maximum displacements and stresses of cross-ply cylindrical shell laminate at S=100 under mechanical loading

Case	$\overline{u_r}\,(0,\frac{\varphi}{2})$			$\overline{\tau_{r\theta}}\,(0,k^*)$			$\overline{\sigma_\theta}\,(\pm\frac{h}{2},\frac{\varphi}{2})$			$\overline{\sigma_x}\,(\pm\frac{h}{2},\frac{\varphi}{2})$		
	Ren [1]	Present	Error (%)	Ren [1]	Present	Error (%)	Ren [1]	Present	Error (%)	Ren [1]	Present	Error (%)
90/0	0.403	0.4012	0.45	0.867	0.867	0	-0.237	-0.2369	0.04	-0.0592	-0.0592	0
							2.158	2.1582	0	0.0216	0.0216	0
90/0/90	0.0787	0.0782	0.64	0.523	0.523	0	-0.786	-0.7866	0.08	-0.0079	-0.0079	0
							0.781	0.7791	0.24	0.0078	0.0078	0

Note: $k^* = \frac{h}{4}$ for case (90/0) and $k^* = 0$ for case (90/0/90)

Table 3
Dimensionless maximum displacements and stresses of cross-ply cylindrical shell laminate at S=4 under thermal loading

Case	$\overline{u_r}\,(\pm\frac{h}{2},\frac{\varphi}{2})$			$\overline{\tau_{r\theta}}\,(0,k^*)$			$\overline{\sigma_\theta}\,(\pm\frac{h}{6},\frac{\varphi}{2})$		
	Ali [8]	Present	Error (%)	Ali [8]	Present	Error (%)	Ali [8]	Present	Error (%)
90/0	76.93	76.93	0	-98.93	-98.93	0	2427.5	2427.6	0
	78.83	78.83	0	-105.9	-102.9	2.9	-1598.95	-1598.95	0
90/0/90	19.6	19.6	0	10.12	10.12	0	-396.9	-396.9	0
	19.75	19.75	0	2.21	2.21	0	347.3	347.3	0

Note: $k^* = 0$ for case (90/0) and $k^* = \pm\frac{h}{6}$ for case (90/0/90)

From Table 2 and 3, it can be noted that the error percentage for two layers and three layers laminate were negligible for displacement and stresses thus validating the formulation for both the mechanical and thermal loading.

3.2 Effect of Material Properties on Thermal Bending

Results based on the developed elasticity solution were generated for different laminate materials to study the effect of material properties, especially coefficient of thermal expansion ratio on cylindrical bending of laminate shells under thermal loading. The three composite materials as in Table 4 were chosen as they are commonly used in aircraft components and also covered a wide range of ratio of coefficient of thermal expansion (3 to 1125).

Table 4
Material Properties of Composite Laminates

Material	$E_L(psi)$	$E_T(psi)$	$G_{LT}(psi)$	$G_{TT'}(psi)$	$\nu_{LT} = \nu_{TT}$	$\frac{\alpha_T}{\alpha_L}$
Graphite/Epoxy	25 x 10^6	1 x 10^6	0.5 x 10^6	0.2 x 10^6	0.25	1125
Kevlar/Epoxy	11.6 x 10^6	0.8 x 10^6	0.31 x 10^6	0.26 x 10^6	0.34	30
Glass/Epoxy	6.5 x 10^6	1.5 x 10^6	0.62 x 10^6	0.5 x 10^6	0.28	3.693

Maximum displacements were often maximum either at top or bottom of laminate while interlaminar stresses were taken at interfaces, so, in Table 5 to Table 7, the displacements were observed at the bottom surface of the laminate while the stresses were observed at the interlaminar surface. Table 5 showed a significant increase in the values of displacements and stresses for Graphite/Epoxy at S=4 (thick laminate) when compared to displacements and stresses at S=100 (thin laminate). This increased value can be attributed to the high ratio of coefficient of thermal expansion of Graphite/Epoxy. No obvious changes in value were observed for Kevlar/Epoxy laminate (Table 6) and Glass/Epoxy laminate (Table 7) as their ratio of coefficient of thermal expansion were lower compared to Graphite/Epoxy.

Table 5
Dimensionless displacements and stresses of Graphite/Epoxy (90/0/90) under thermal loading

S	Graphite/Epoxy				
	$\overline{u_r}$ (-h/2)	$\overline{u_\theta}$ (-h/2)	$\overline{\sigma_\theta}$ (h/6)	$\overline{\tau_{r\theta}}$ (h/6)	$\overline{\sigma_r}$ (h/6)
4	19.75	5.388	-396.9	10.12	-11.4
20	3.828	1.3	-377.7	1.687	-0.6587
100	3.175	1.049	-372.6	0.3069	-0.1

Table 6
Dimensionless displacements and stresses of Kevlar/Epoxy (90/0/90) under thermal loading

S	Kevlar/Epoxy				
	$\overline{u_r}$ (-h/2)	$\overline{u_\theta}$ (-h/2)	$\overline{\sigma_\theta}$ (h/6)	$\overline{\tau_{r\theta}}$ (h/6)	$\overline{\sigma_r}$ (h/6)
4	0.8991	0.3604	-10.34	0.2595	-0.2334
20	0.4215	0.1582	-9.766	0.0435	-0.0162
100	0.402	0.1334	-9.631	0.0079	-0.0026

Table 7
Dimensionless displacements and stresses of Glass/Epoxy (90/0/90) under thermal loading

S	Glass/Epoxy				
	$\overline{u_r}$ (-h/2)	$\overline{u_\theta}$ (-h/2)	$\overline{\sigma_\theta}$ (h/6)	$\overline{\tau_{r\theta}}$ (h/6)	$\overline{\sigma_r}$ (h/6)
4	0.3467	0.1981	-0.9659	0.022	-0.0123
20	0.2919	0.1126	-0.9235	0.0039	-0.0014
100	0.2897	0.9627	-0.9158	0.0007	-0.0002

Further observation can be made on the displacements and interlaminar stresses of the (90/0/90) laminated shell made of different composite materials. Figure 2, 4, 6, 8 and 10 compared the behaviour of the three different composite laminates under mechanical loading while Figure 3, 5, 7, 9 and 11 compared the behaviour of the three different composite laminate under thermal loading. It is to be noted that for the vertical axis of the graphs, *2(r-R)/h* was used to convert the arbitrary

radius into numerical values ranging from -1 (bottom surface) to +1 (top surface). *r* referred to the radius of current layer studied while *R* referred to the mean radius. *h* indicated the total thickness of the laminate shell.

Figure 2 to Figure 5 showed displacements in r and θ direction for the laminate shells made of different materials. From the figures it can be observed that under mechanical loading, Glass/Epoxy experienced the highest displacement in both *r* and θ direction. This was due to Glass/Epoxy's small modulus of elasticity. Glass/Epoxy had the least resistance to elastic deformation compared to the other two materials.

However, when thermal load was applied, Graphite/Epoxy experienced significant nonlinearity and had the highest displacement in both *r* and θ direction. Graphite/Epoxy had the highest ratio of coefficient of thermal expansion among the materials, and this high ratio played an important role in the behaviour of composite laminated shell under thermal loading. For thermal loading, Figure 3 showed the remarkable non-linear variation for $\bar{u}_r$, which reveals that there was a normal strain in the direction r which could not be neglected for thick laminate made of material with high ratio of coefficient of thermal expansion. This variation was termed as "thickness stretch" which was completely absent in mechanical loading and also for Glass/Epoxy and Kevlar/Epoxy under thermal loading. Elasticity solutions serve as a benchmark and gave a guideline for researchers to select a model for approximate analysis [8]. Thus, one has to be careful in adding this "thickness stretch" term in any higher order model for thermal loading to have accurate results.

In Figure 4 and 5, a zig zag pattern of in-plane displacement was observed for Graphite/Epoxy for both mechanical and thermal load. The zig zag pattern was clearly obvious for Graphite/Epoxy due to its high ratio of elasticity modulus (E_L/E_T). Thus, while selecting a model for approximate analysis [8], one has to be careful in adding a "Murakami zig-zag" function as in Ali *et al.,* [8], for both mechanical and thermal loading to have accurate results.

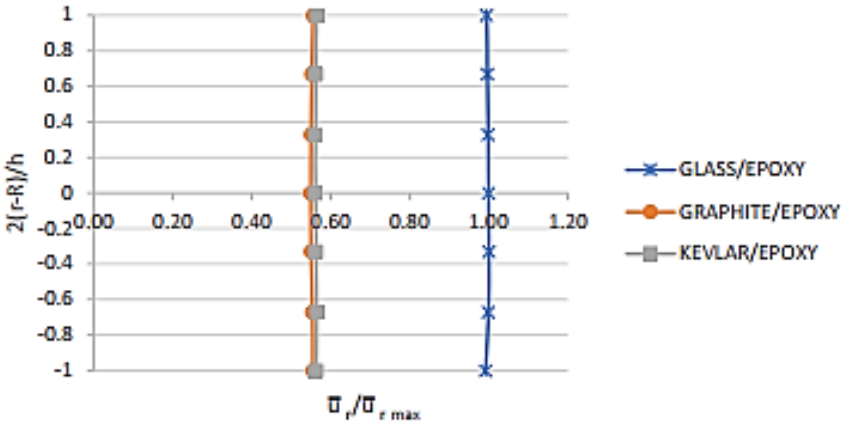

Fig. 2. Variation of $\bar{u}_r$ for laminated shells (90/0/90) for mechanical loading at S=4

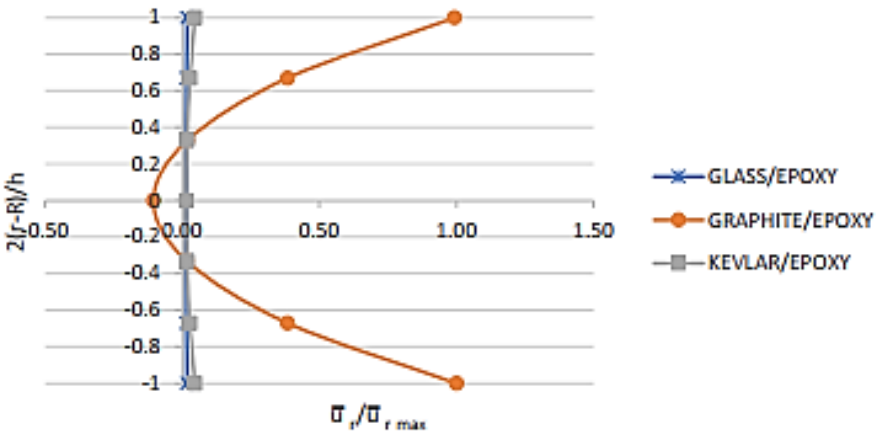

Fig. 3. Variation of $\bar{u}_r$ for laminated shells (90/0/90) for thermal loading at S=4

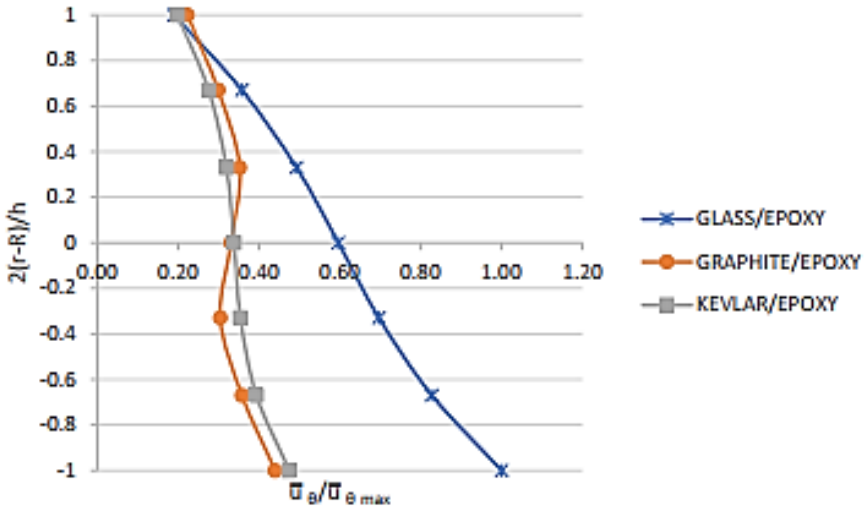

Fig. 4. Variation of $\bar{u}_\theta$ for laminated shells (90/0/90) for mechanical loading at S=4

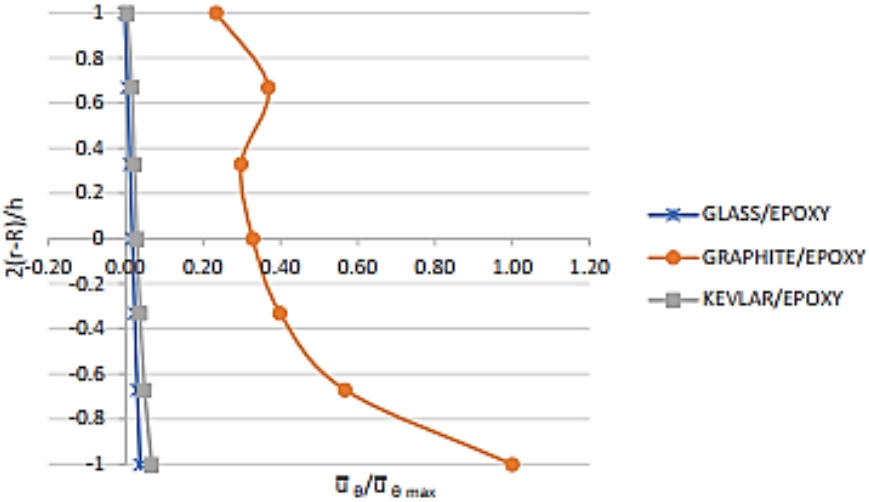

Fig. 5. Variation of $\bar{u}_\theta$ for laminated shells (90/0/90) for thermal loading at S=4

Figure 6 to 11 showed thickness-wise variation for in-plane shear and normal stresses in r and θ direction for the laminate shells with different materials. It was observed that for material with high ratio of coefficient of thermal expansion (Graphite/Epoxy), thermal load affected the stresses more than the mechanical load. Thickness stretch effect became more pronounced hence in-plane shear and stresses in r and θ direction increased prominently especially in the midplane of laminate for mechanical loading and maximum at the interfaces of the laminate for thermal loading.

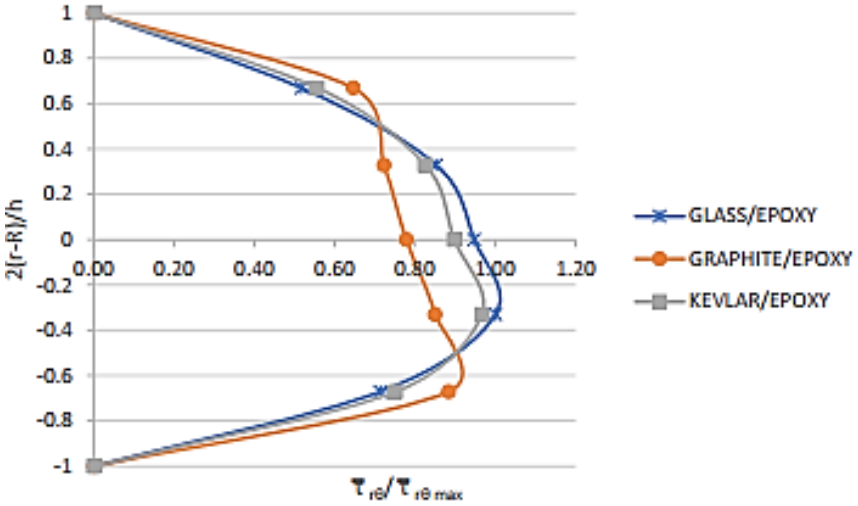

Fig. 6. Variation of $\bar{\tau}_{r\theta}$ of laminated shells (90/0/90) for mechanical loading at S=4

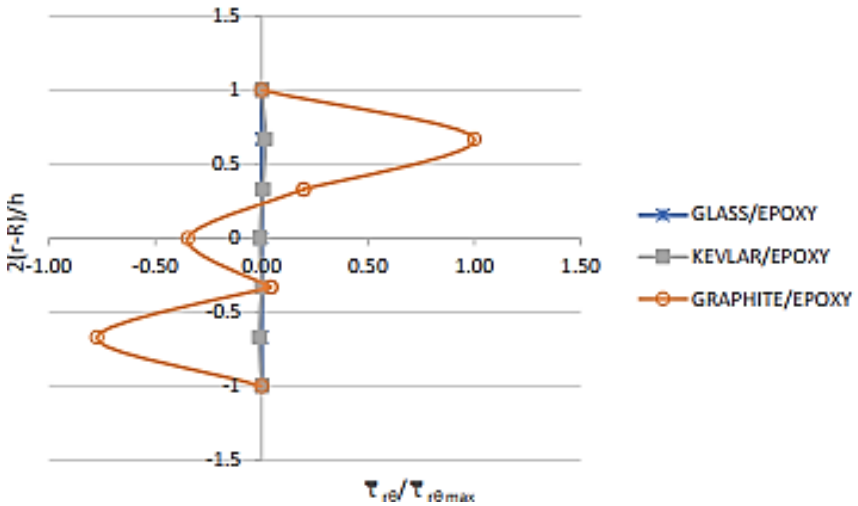

Fig. 7. Variation of $\bar{\tau}_{r\theta}$ of laminated shells (90/0/90) for thermal loading at S=4

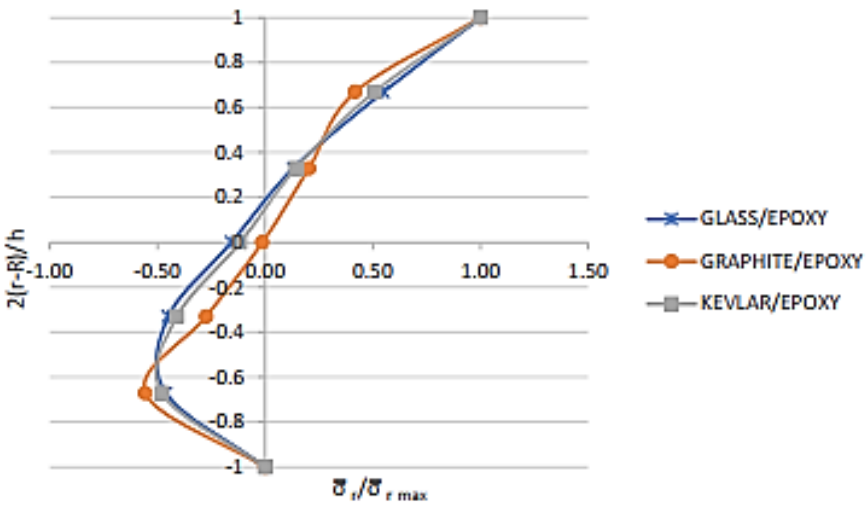

Fig. 8. Variation of $\bar{\sigma}_r$ of laminated shells (90/0/90) for mechanical loading at S=4

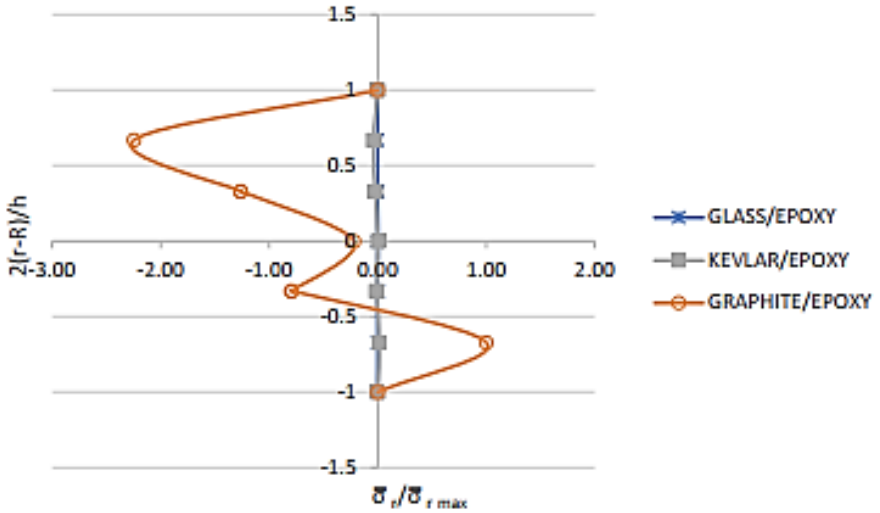

Fig. 9. Variation of $\bar{\sigma}_r$ of laminated shells (90/0/90) for thermal loading at S=4

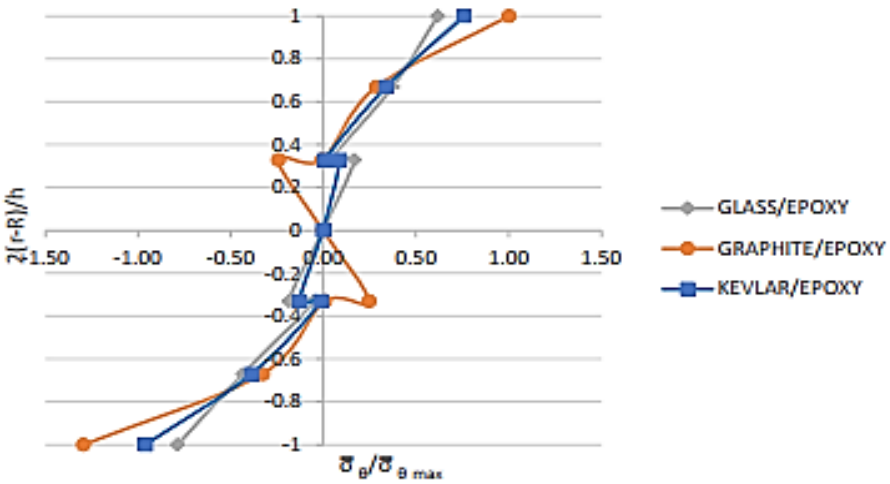

Fig. 10. Variation of $\bar{\sigma}_\theta$ of laminated shells (90/0/90) for mechanical loading at S=4

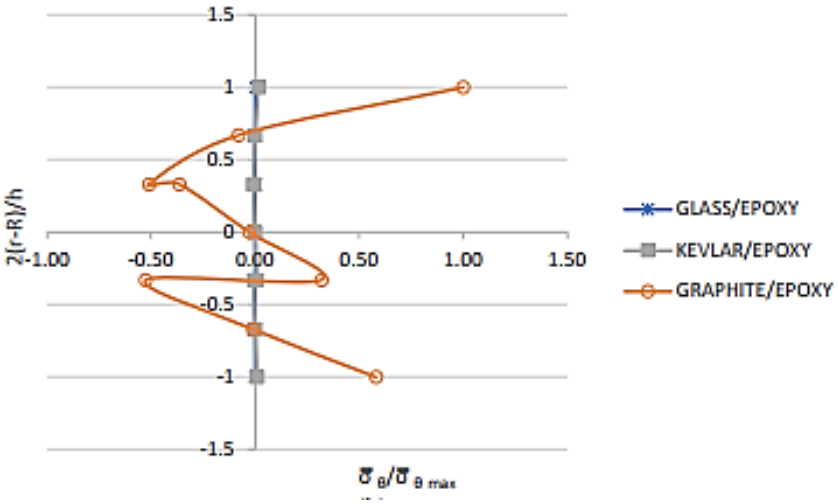

Fig. 11. Variation of $\bar{\sigma}_\theta$ of laminated shells (90/0/90) for thermal loading at S=4

From Figure 10 and 11, it was noted that for both mechanical and thermal loading the maximum stress occurred at the top surface of the laminate and again the Graphite/Epoxy laminates under thermal loading proved to be critical.

As Graphite/Epoxy showed the most prominent curves, the comparison between the behaviour of Graphite/Epoxy laminate under mechanical and thermal loading was further made. Figure 12 and 13 further emphasized the nonlinearity of displacements of thick laminate shell when it was under thermal loading. Maximum displacements were recorded when thermal load was applied to the laminate. It was very obvious from Figure 12 as discussed earlier, the thickness stretch effect was present only for mechanical loading whereas the zigzag nature of in plane displacement as depicted in Figure 13 was present for both mechanical and thermal loading.

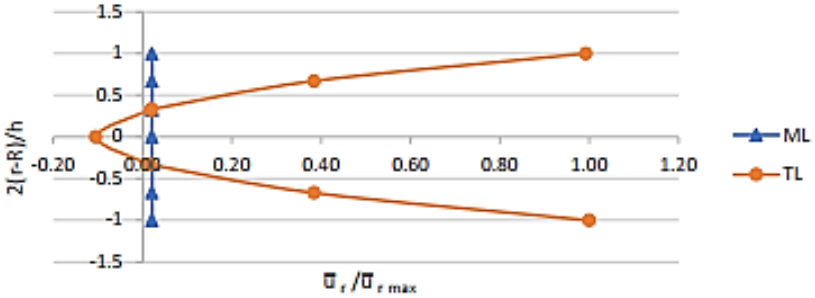

Fig. 12. Comparison of $\bar{u}_r$ of Graphite/Epoxy laminated shells (90/0/90) for mechanical (ML) and thermal loading (TL) at S=4

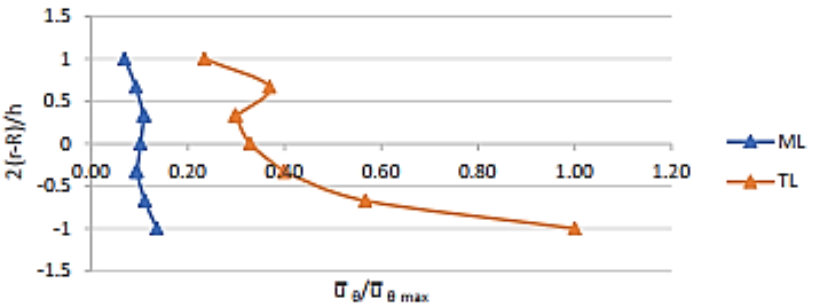

Fig. 13. Comparison of $\bar{u}_\theta$ of Graphite/Epoxy laminated shells (90/0/90) for mechanical (ML) and thermal loading (TL) at S=4

4. Conclusions

The elasticity solution based on three-dimensional linear uncoupled thermo-elasticity for cylindrical bending of simply supported laminated composite shells under thermo-mechanical loading has been developed. The effect of material properties on the behaviour of laminate cylindrical shell had been studied. From the analysis of different materials, it can be concluded that thermal loading caused the thickness-stretch effect to be more pronounced in thick laminates and even more so when the material had high thermal coefficient expansion ratio such as Graphite/Epoxy laminates. This thickness stretch effect was not seen for thin laminates and for Boron/Epoxy and Kevlar/Epoxy because of their low coefficient of thermal expansion ratio. Moreover, for mechanical loading thickness stretch effect was obviously absent whereas the in-plane displacement zig-zag effect (interface discontinuity) was more pronounced.

Based on the benchmark elasticity solution it can be concluded that while selecting an approximate two-dimensional model to analyse the bending of a composite laminated shell under thermal loading, one should consider the laminate thickness and the thermal expansion coefficient ratio of the composite laminate to avoid erroneous results. Based on the present analysis, it can be concluded that any higher order shear deformation model that includes higher order terms in deflection to consider the thickness stretch effect and an inclusion of zig-zag term in the in-plane displacements will be good for accurate analysis of any thick composite laminates under thermo-mechanical loading.

Acknowledgement
This research was supported by Ministry of Education of Malaysia (MOE) through Fundamental Research Grant Scheme (FRGS/1/2022/TK04/UIAM/02/14).

Reference

[1] Ren, J. G. "Exact solutions for laminated cylindrical shells in cylindrical bending." *Composites Science and Technology* 29, no. 3 (1987): 169-187. https://doi.org/10.1016/0266-3538(87)90069-8
[2] Huang, N. N., and T. R. Tauchert. "Thermoelastic solution for cross-ply cylindrical panels." *Journal of thermal stresses* 14, no. 2 (1991): 227-237. https://doi.org/10.1080/01495739108927064
[3] Huang, N. N., and T. R. Tauchert. "Thermal stresses in doubly-curved cross-ply laminates." *International Journal of Solids and Structures* 29, no. 8 (1992): 991-1000. https://doi.org/10.1016/0020-7683(92)90070-A
[4] Khdeir, A. A. "Thermoelastic analysis of cross-ply laminated circular cylindrical shells." *International Journal of Solids and Structures* 33, no. 27 (1996): 4007-4017. https://doi.org/10.1016/0020-7683(95)00229-4
[5] Bhaskar, K., T. K. Varadan, and J. S. M. Ali. "Thermoelastic solutions for orthotropic and anisotropic composite laminates." *Composites Part B: Engineering* 27, no. 5 (1996): 415-420. https://doi.org/10.1016/1359-8368(96)00005-4
[6] Khare, Rakesh Kumar, Tarun Kant, and Ajay Kumar Garg. "Closed-form thermo-mechanical solutions of higher-order theories of cross-ply laminated shallow shells." *Composite Structures* 59, no. 3 (2003): 313-340. https://doi.org/10.1016/S0263-8223(02)00245-3
[7] Qian, Hai, Ding Zhou, Weiqing Liu, Hai Fang, and Weidong Lu. "Elasticity solutions of simply supported laminated cylindrical arches subjected to thermo-loads." *Composite Structures* 131 (2015): 273-281. https://doi.org/10.1016/j.compstruct.2015.04.052
[8] Mohamed Ali, J. S., Saleh Alsubari, and Yulfian Aminanda. "Hygrothermoelastic analysis of orthotropic cylindrical shells." *Latin American Journal of Solids and Structures* 13 (2016): 573-589. https://doi.org/10.1590/1679-78252249
[9] Liu, Bo, Shuai Lu, Jinzu Ji, A. J. M. Ferreira, Cuiyun Liu, and Yufeng Xing. "Three-dimensional thermo-mechanical solutions of cross-ply laminated plates and shells by a differential quadrature hierarchical finite element method." *Composite Structures* 208 (2019): 711-724. https://doi.org/10.1016/j.compstruct.2018.10.022
[10] Kumari, Poonam, and Shranish Kar. "Static behavior of arbitrarily supported composite laminated cylindrical shell panels: an analytical 3D elasticity approach." *Composite Structures* 207 (2019): 949-965 https://doi.org/10.1016/j.compstruct.2018.09.035.

[11] Kar, Shranish, and Poonam Kumari. "A 3D solution for angle-ply cylindrical shell panel supported arbitrarily on its boundaries using extended Kantorovich method." *International Journal of Advances in Engineering Sciences and Applied Mathematics* 12 (2020): 51-64. https://doi.org/10.1007/s12572-020-00267-5

[12] Wu, Yang, Yufeng Xing, and Bo Liu. "Analysis of isotropic and composite laminated plates and shells using a differential quadrature hierarchical finite element method." *Composite Structures* 205 (2018): 11-25. https://doi.org/10.1016/j.compstruct.2018.08.095

[13] Roy, Soumen, Sandipan Nath Thakur, and Chaitali Ray. "A modified higher order zigzag theory for response analysis of doubly curved cross-ply laminated composite shells." *Mechanics of Advanced Materials and Structures* 29, no. 26 (2022): 5026-5040.

[14] Thakur, Sandipan Nath, and Chaitali Ray. "Static and free vibration analyses of moderately thick hyperbolic paraboloidal cross ply laminated composite shell structure." In *Structures*, vol. 32, pp. 876-888. Elsevier, 2021. https://doi.org/10.1016/j.istruc.2021.03.066

[15] Kappel, Andreas, and Christian Mittelstedt. "Interlaminar stress fields in circular cylindrical cross-ply laminated shells subjected to transverse loadings." *International Journal of Solids and Structures* 228 (2021): 111096. https://doi.org/10.1016/j.ijsolstr.2021.111096

[16] Chandrashekhara, K., and A. Bhimaraddi. "Thermal stress analysis of laminated doubly curved shells using a shear flexible finite element." *Computers & structures* 52, no. 5 (1994): 1023-1030. https://doi.org/10.1016/0045-7949(94)90086-8

[17] Dhepe, Sharvari N., Abhay N. Bambole, and Yuwaraj M. Ghugal. "An elasticity solution of laminated cylindrical panel." *Forces in Mechanics* 9 (2022): 100147.

[18] Alibeigloo, A., and M. Shakeri. "Elasticity solution for static analysis of laminated cylindrical panel using differential quadrature method." *Engineering structures* 31, no. 1 (2009): 260-267. https://doi.org/10.1016/j.engstruct.2008.08.012

[19] Biswal, M., S. K. Sahu, and A. V. Asha. "Vibration of composite cylindrical shallow shells subjected to hygrothermal loading-experimental and numerical results." *Composites Part B: Engineering* 98 (2016): 108-119. https://doi.org/10.1016/j.compositesb.2016.05.037

[20] Amoushahi, Hossein, and Farshad Goodarzian. "Dynamic and buckling analysis of composite laminated plates with and without strip delamination under hygrothermal effects using finite strip method." *Thin-Walled Structures* 131 (2018): 88-101. https://doi.org/10.1016/j.tws.2018.06.030